Electronic Supplementary Information

Chiral Molecular Nanosilicas

Zhaohui Zong,[a] Aiyou Hao,[a] Pengyao Xing*[,a,b] and Yanli Zhao*[b]

[a]*Key Laboratory of Colloid and Interface Chemistry of Ministry of Education and School of Chemistry and Chemical Engineering, Shandong University, Jinan 250100, People's Republic of China.*

[b]*Division of Chemistry and Biological Chemistry, School of Physical and Mathematical Sciences, Nanyang Technological University, 21 Nanyang Link, Singapore 637371, Singapore.*

Email: xingpengyao@sdu.edu.cn; zhaoyanli@ntu.edu.sg

Experimental section

Materials

1,1'-Ferrocnedocarboxylic acid and all amino acid methyl ester hydrochlorides were purchased from HEOWNS Biochemical Technology Co., LTD, China. POSS-NH_2 was purchased from Xi'an Qiyue Biological Technology Co., Ltd. All reagents were used without further purification in this work. *L*-Configuration amino acids are used throughout this supporting information unless otherwise specified.

Characterizations

^{1}H NMR spectra, ^{13}C NMR spectra and temperature-variable ^{1}H NMR spectra were collected by BRUKER AVANCE III HD 400. High-Resolution Mass Spectra (HR-MS) were performed on an Agilent Q-TOF 6510. Circular dichroism (CD) spectra, temperature-variable CD spectra and solid CD spectra were measured with an Applied Photophysics ChirascanV100 model. Vibrational circular dichroism (VCD) spectra were obtained by a JASCO FVS-6000. VCD testing parameters: data interval: 1.92847 cm^{-1}; IR accumulation: 16; VCD accumulation: 6000;

resolution: 8 cm^{-1}; scanning speed: 4 mm/sec; polarizer angle: -45°; cell length: 50 μm. Transmission electron microscope (TEM) images were measured on a HITACHI HT-7700. The samples for TEM detection were dropped in the copper grid and air-dried. Scanning Electron Microscopy (SEM) images were obtained by Carl Zeiss G300 FE-SEM System. The samples for SEM detection were dropped on the silicon wafers and air-dried. Atomic force microscopy (AFM) testing was conducted with a Bruker Bioscope Resolve and operated in tapping mode at ambient temperature. The AFM samples were dropped on the mica wafer and dried. Single crystal data were collected on a Rigaku XtaLAB Synergy. Powder X-ray diffraction (XRD) patterns were collected on a German Bruker/D8 Advanced diffractometer with Cu Kα radiation (λ = 0.15406 nm, voltage 40 KV, current 40 mA). The samples for XRD were casted onto cover glasses (18 mm × 18 mm) and dried to form thin films.

Solid-state CD spectra

To obtain solid samples, building units were dissolved in CH_2Cl_2, followed by air-drying. The solid samples were then mixed in a mortar with KBr (5 mg solid sample in 200 mg KBr) under an infrared lamp. The ground mixtures were tableted into transparent tablets and tested.

Computational details

The geometric conformations of the molecules (Val-POSS, Met-POSS, Phe-POSS) used in the calculations were obtained from the corresponding single crystals. Then optimization to the energy-minimum structure in the gas phase was performed using Gaussian16 software with B3LYP/6-31g level of theory. Based on the optimized geometry, vibrational circular dichroism (VCD) spectra and electronic circular dichroism (ECD) spectra were calculated to obtain with basic set of B3LYP/6-311g. The geometric conformation of Glu-POSS was built in Gaussian View 06 and then optimized to the energy-minimum structure using Gaussian 16 software. The basis set used in the optimization process was B3LYP/6-31g. Vibrational circular dichroism (VCD) spectrum and electronic circular dichroism (ECD) spectrum were calculated based on the above pre-settings.

In the optimization process, the convergence criteria of optimization were as follows: Maximum Force 0.000015, RMS Force 0.000010, Maximum Displacement 0.000060, RMS

Displacement 0.000040. To ensure that the optimized geometry was at a minimum, all geometry optimizations were followed by a frequency calculation and only positive frequencies were obtained.

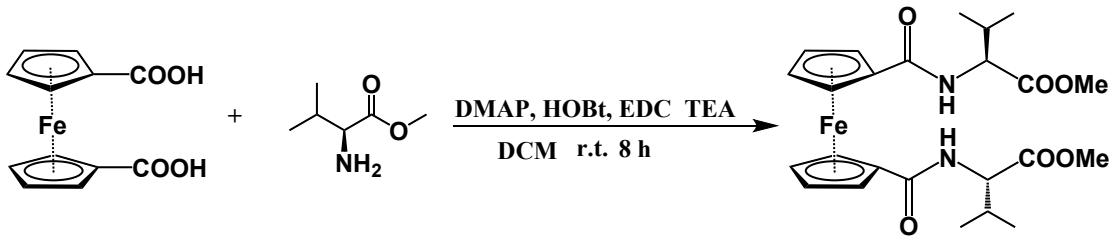

Scheme S1. Synthesis route of ferrocene diamino acid methyl ester.

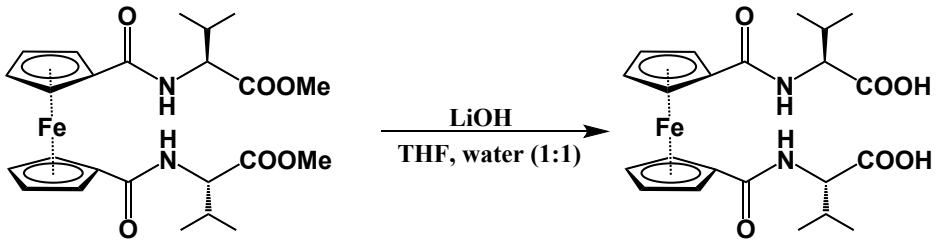

Scheme S2. Synthesis route of ferrocene diamino acid.

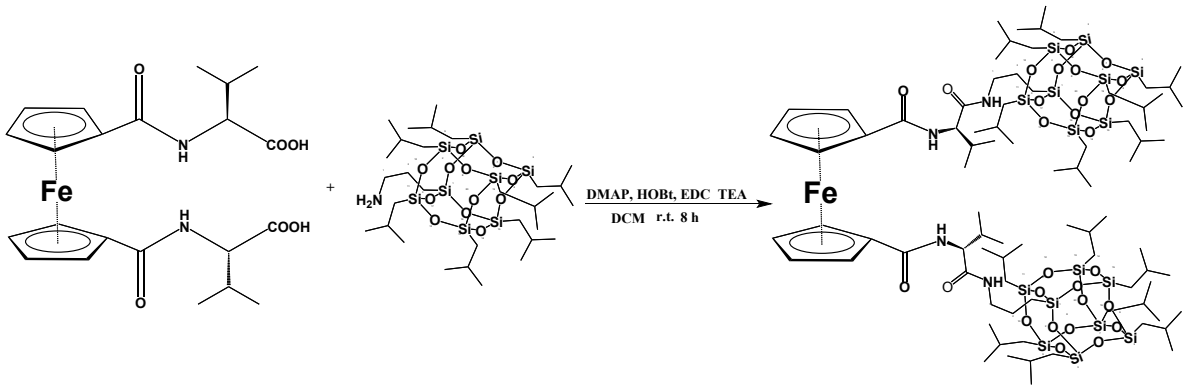

Scheme S3. Synthesis route of Val-POSS.

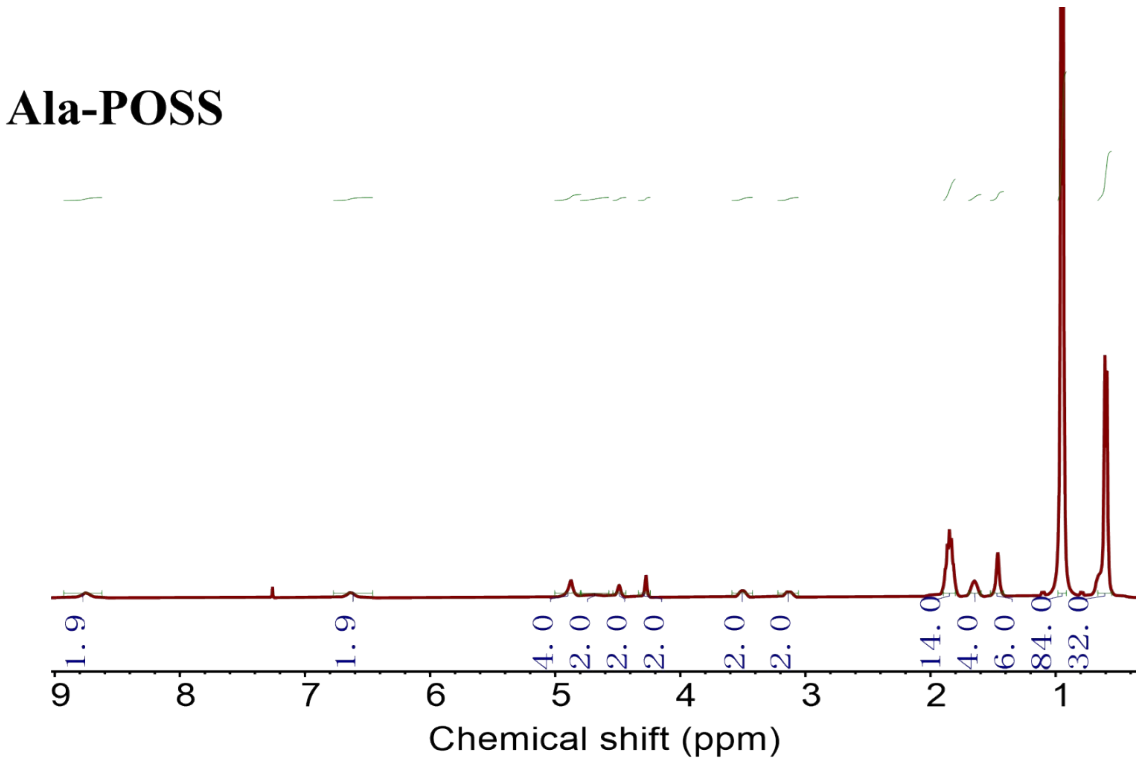

Figure S1. ^{1}H NMR spectrum of Ala-POSS.

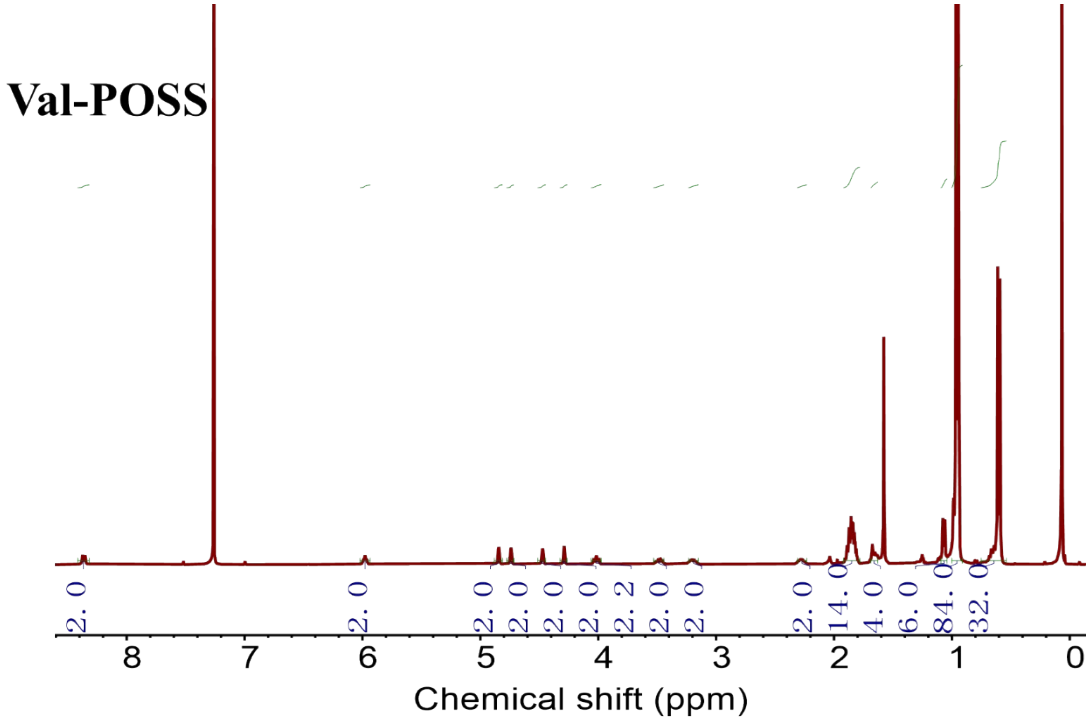

Figure S2. ^{1}H NMR spectrum of Val-POSS.

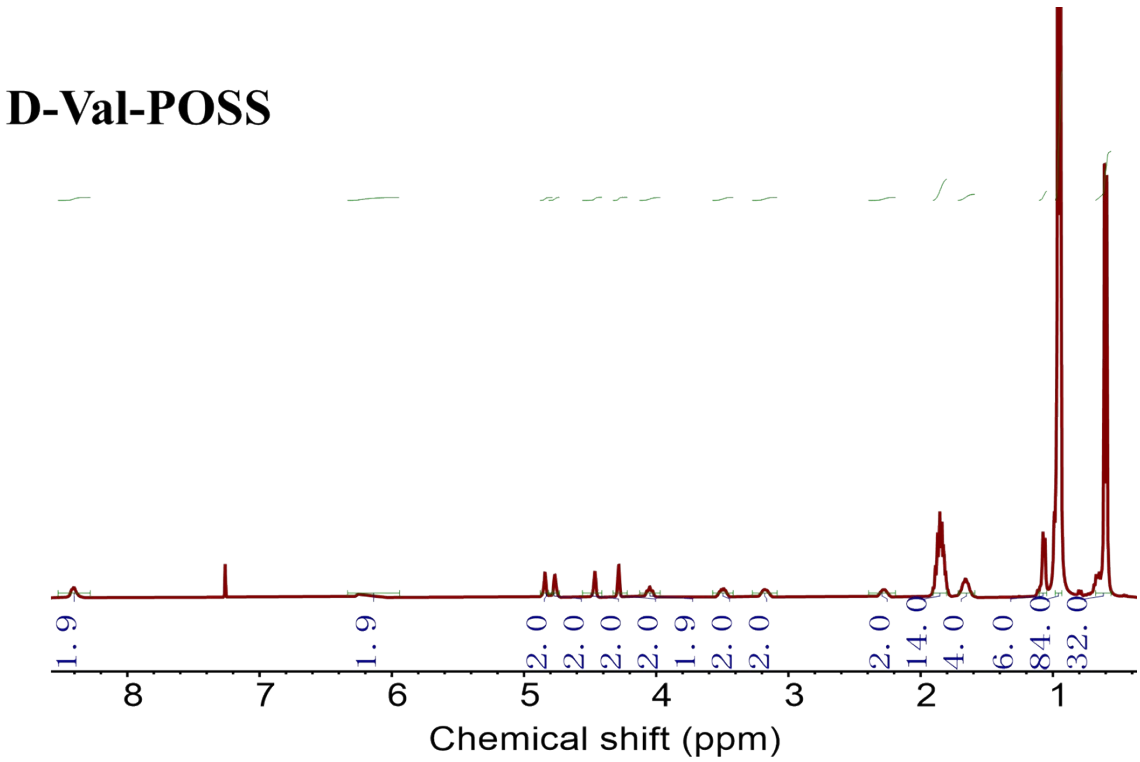

Figure S3. ^{1}H NMR spectrum of D-Val-POSS.

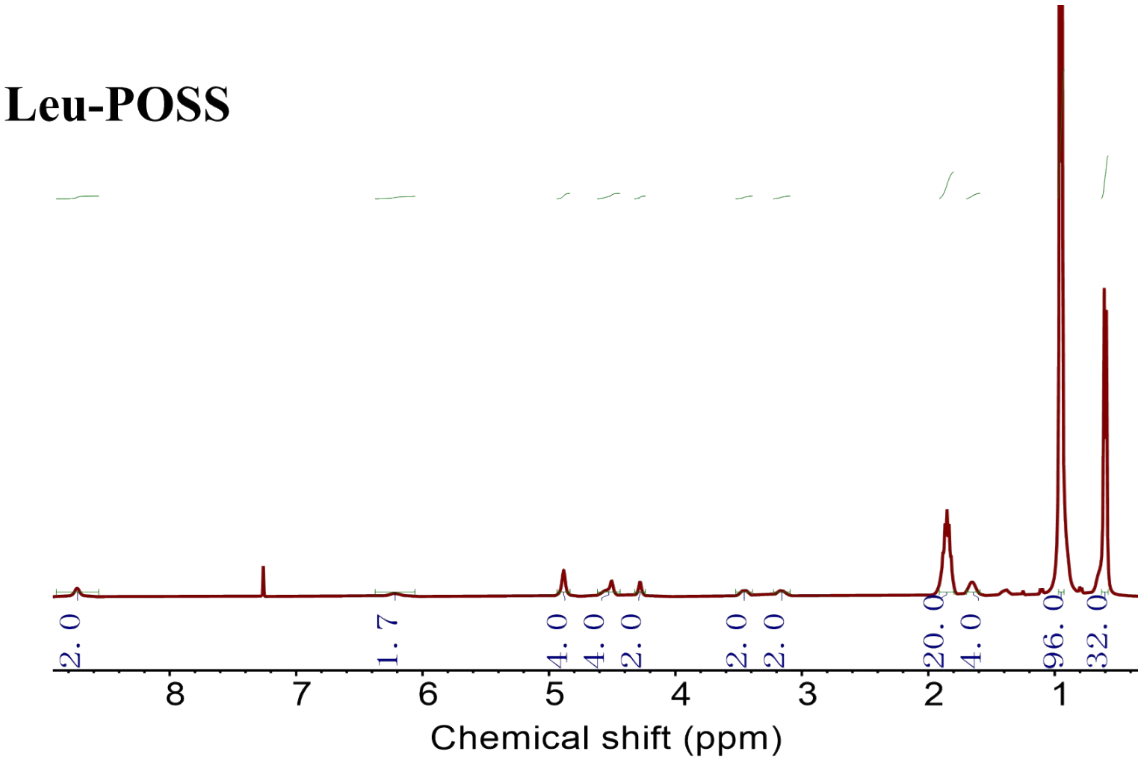

Figure S4. ^{1}H NMR spectrum of Leu-POSS.

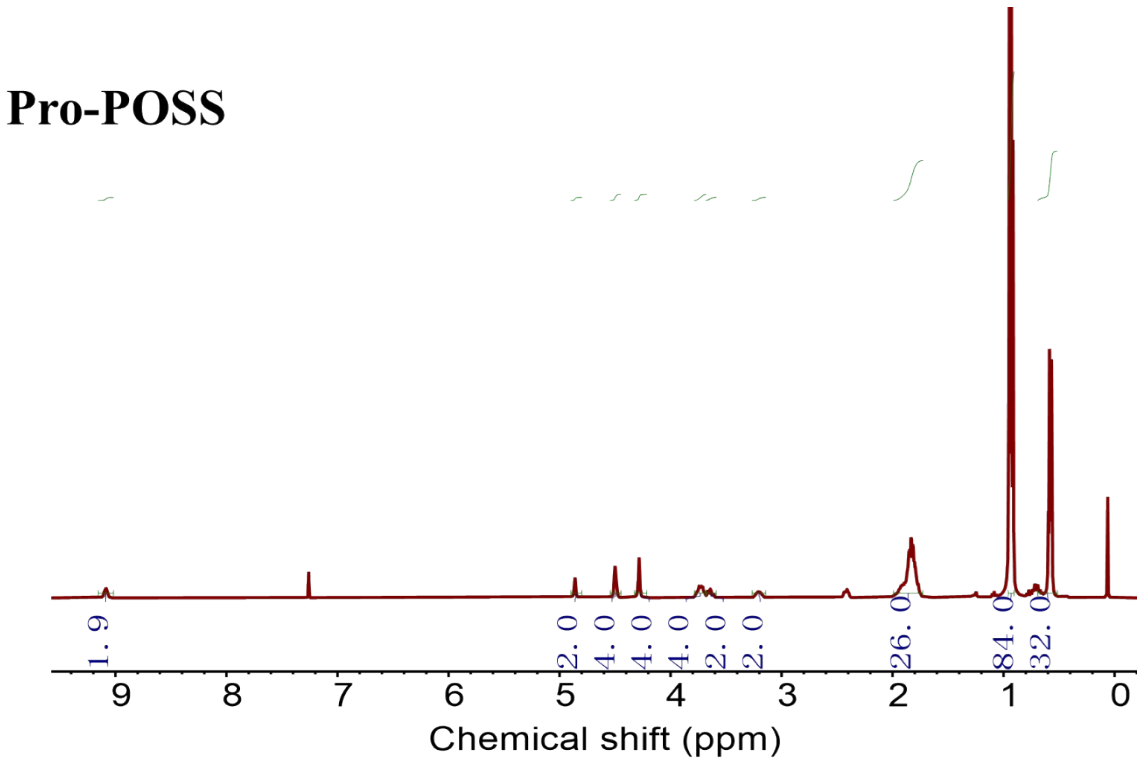

Figure S5. ^{1}H NMR spectrum of Pro-POSS.

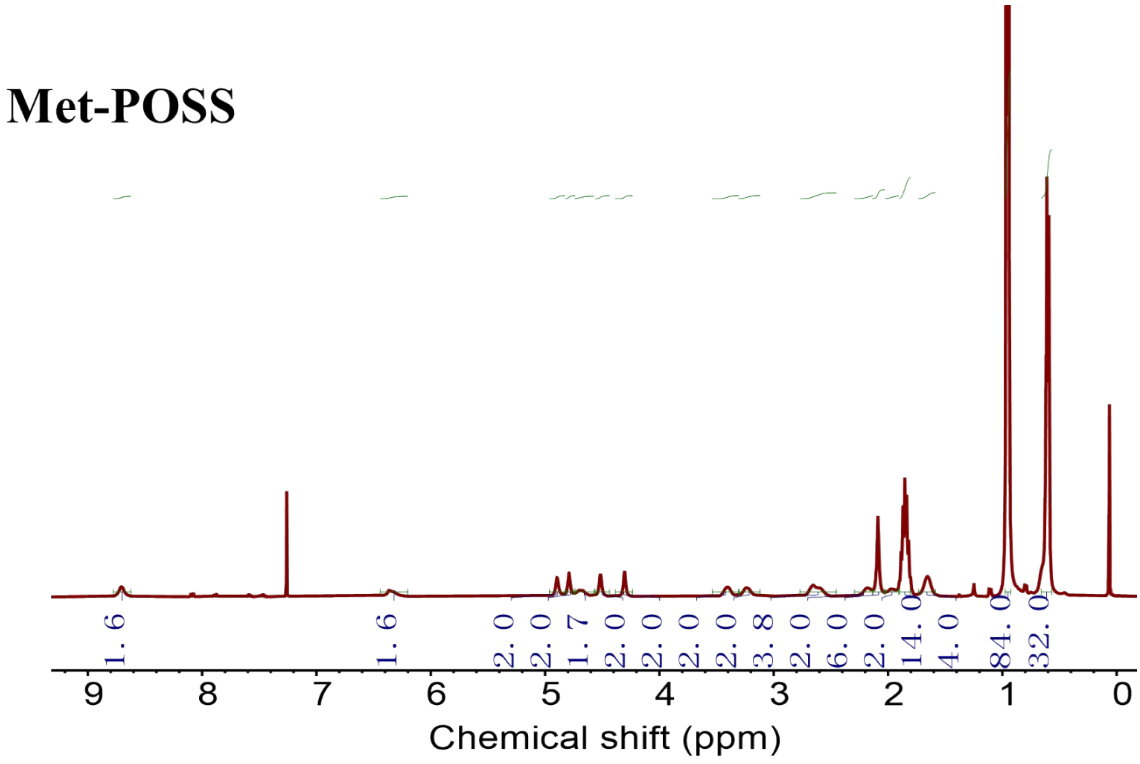

Figure S6. ^{1}H NMR spectrum of Met-POSS.

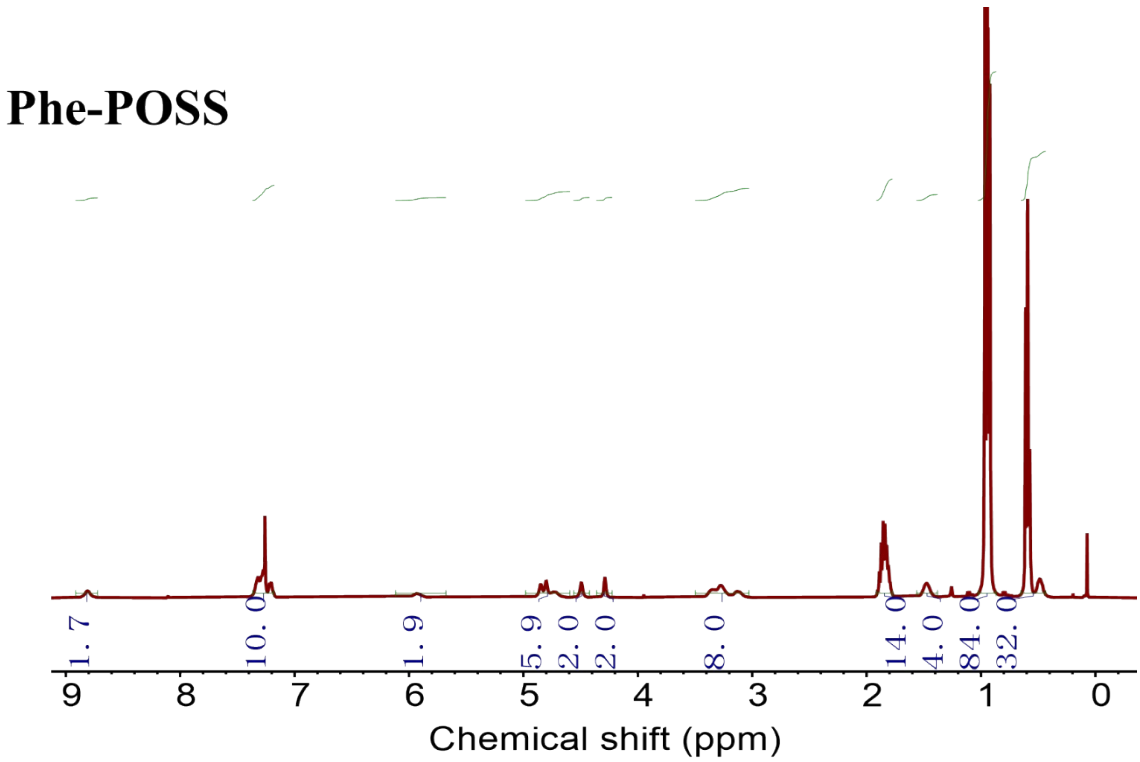

Figure S7. ^{1}H NMR spectrum of Phe-POSS.

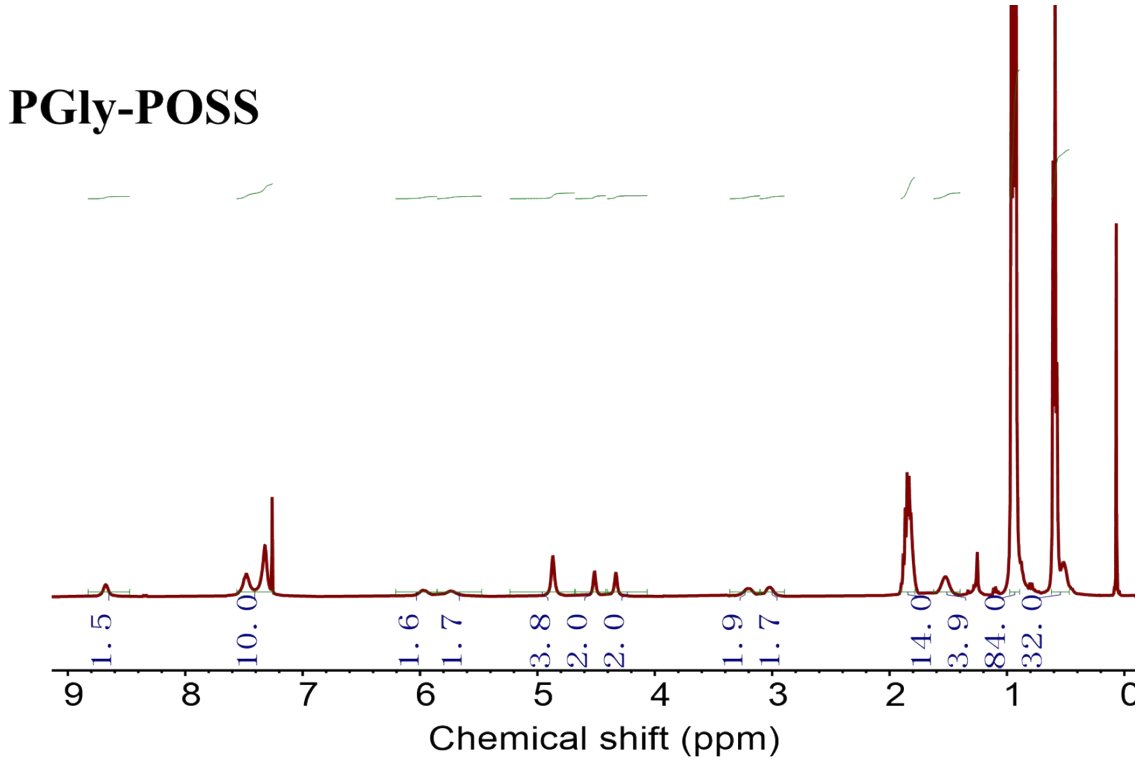

Figure S8. ^{1}H NMR spectrum of PGly-POSS.

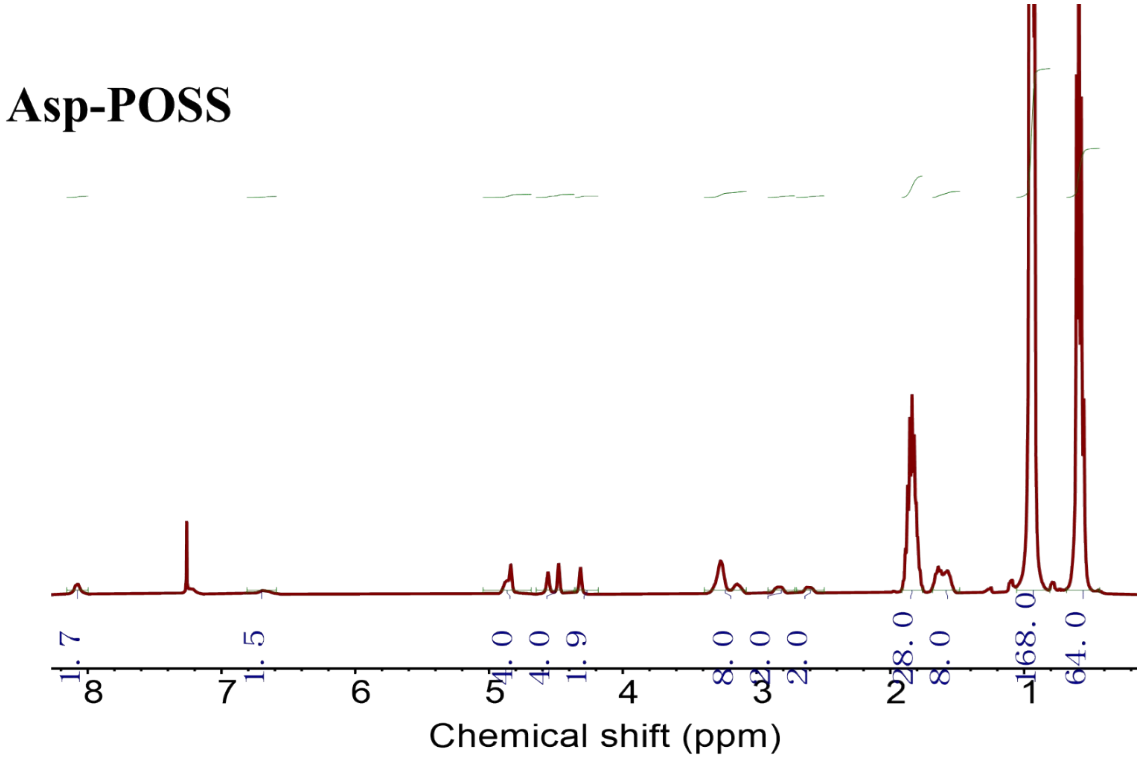

Figure S9. ^{1}H NMR spectrum of Asp-POSS.

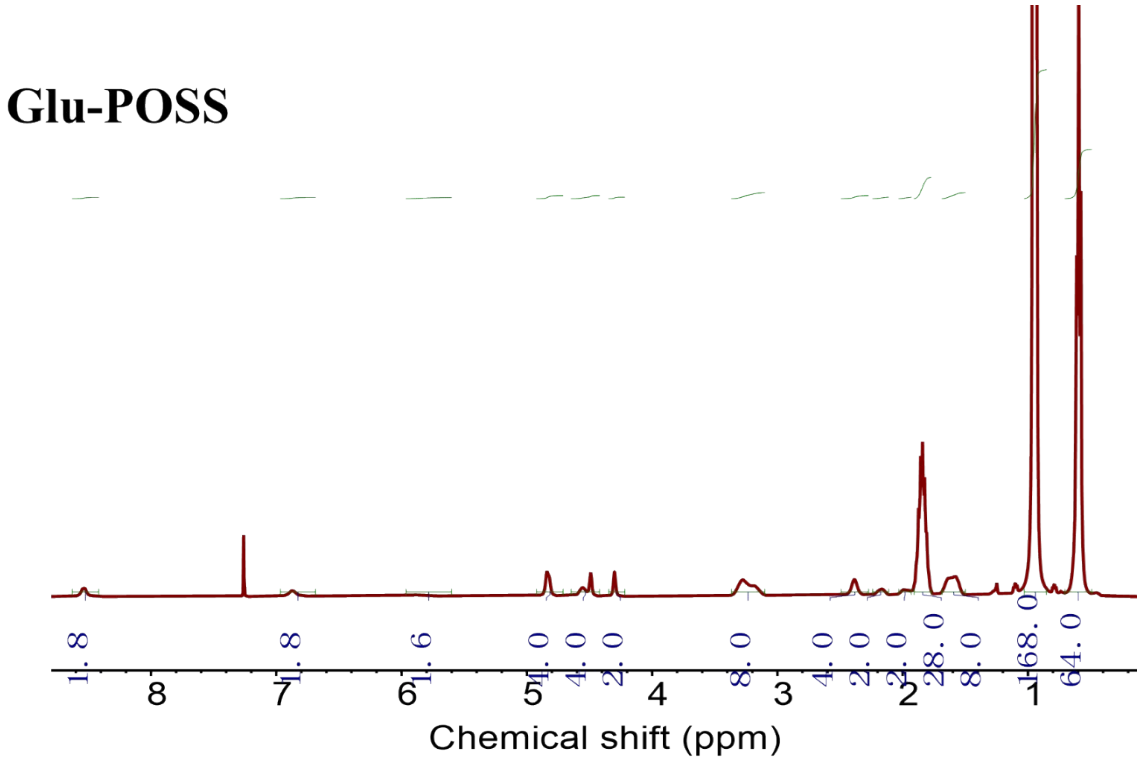

Figure S10. ^{1}H NMR spectrum of Glu-POSS.

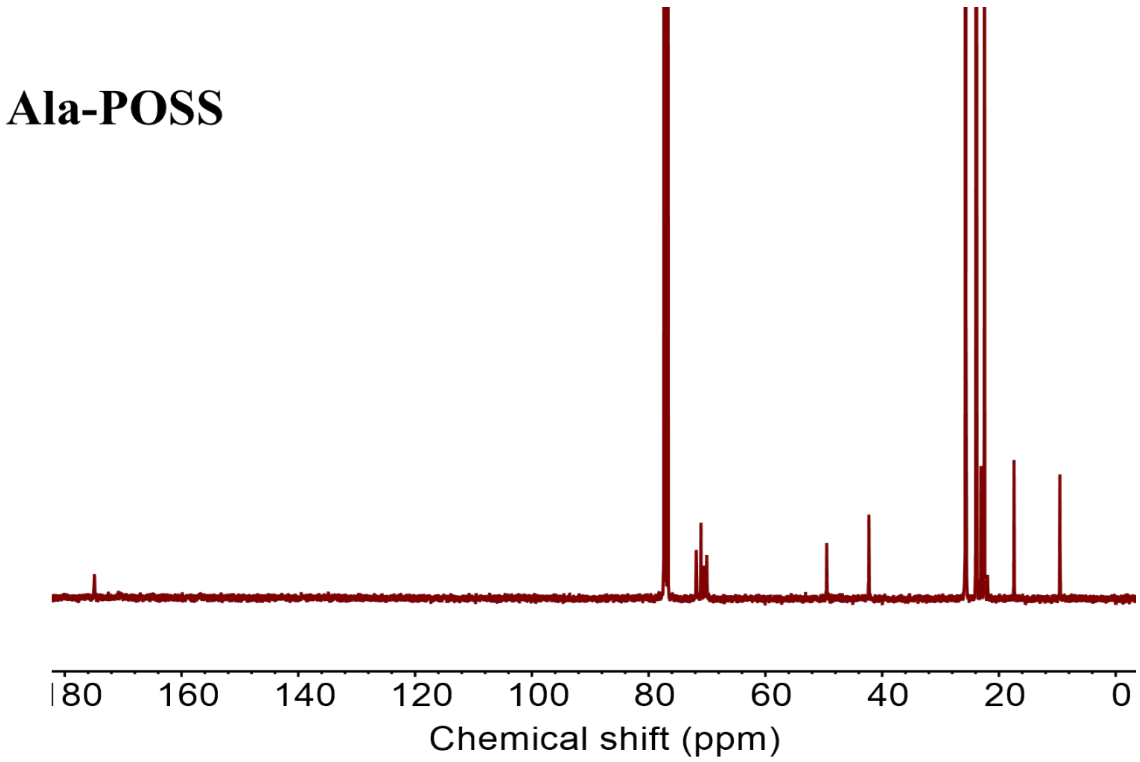

Figure S11. ^{13}C NMR spectrum of Ala-POSS.

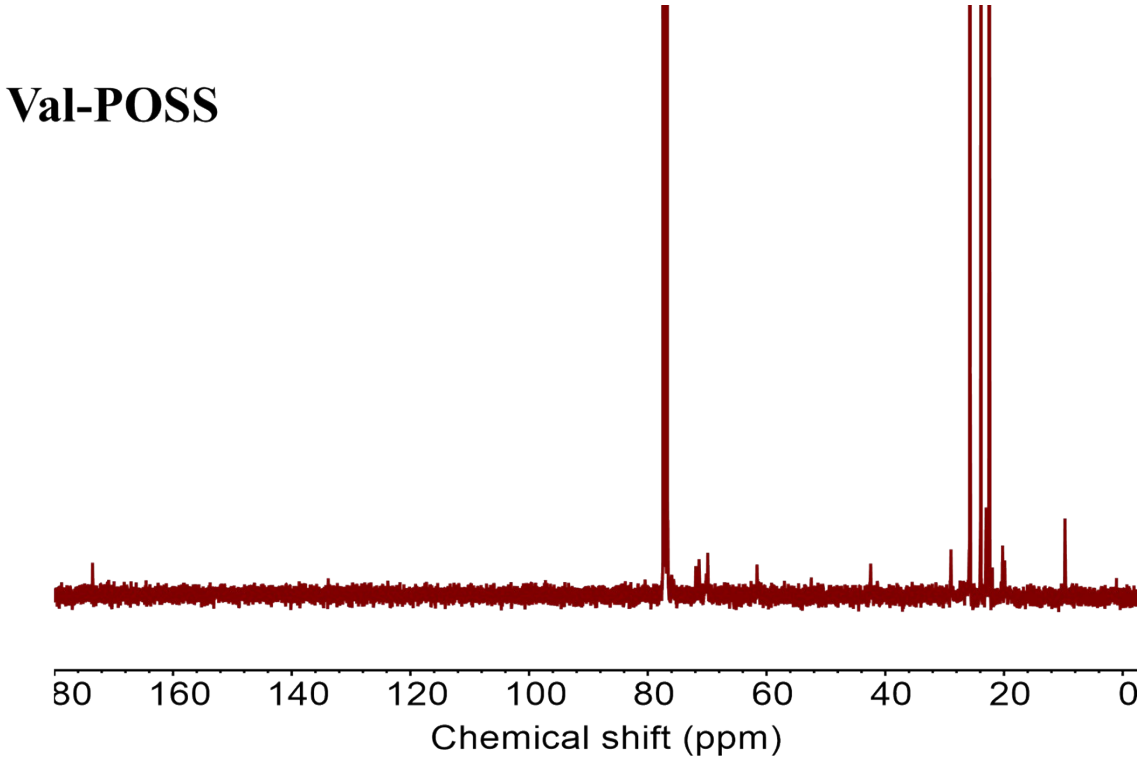

Figure S12. ^{13}C NMR spectrum of Val-POSS.

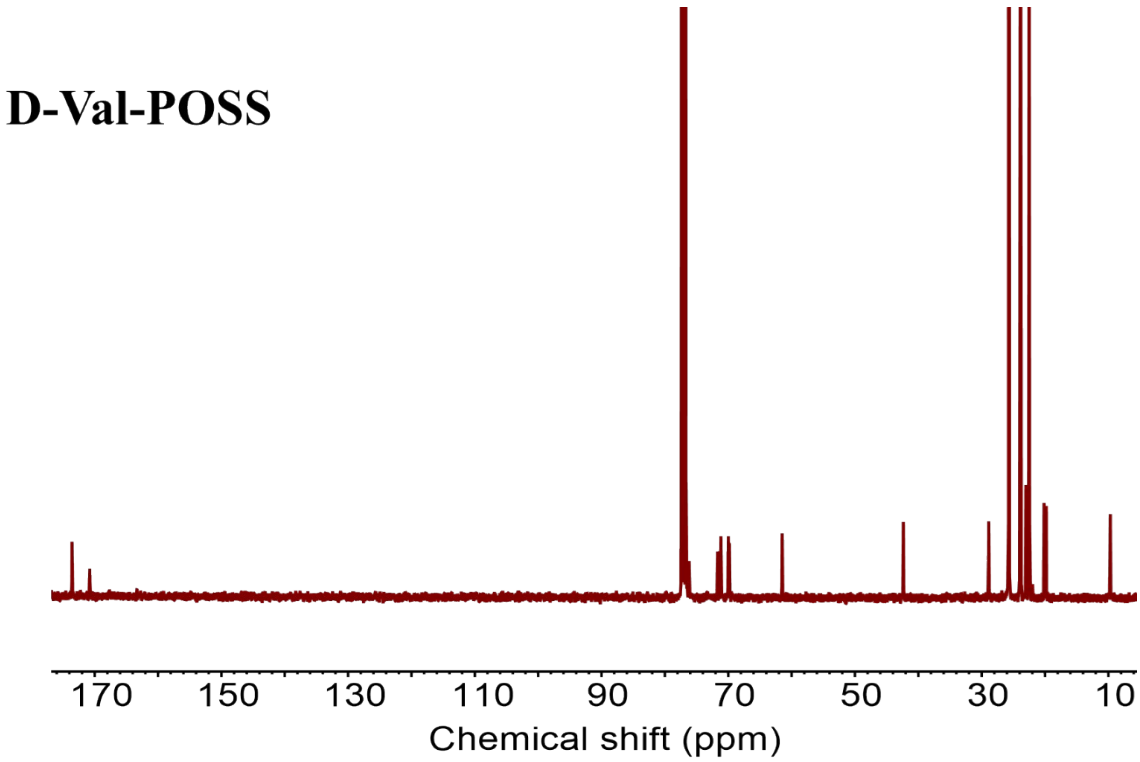

Figure S13. ^{13}C NMR spectrum of D-Val-POSS.

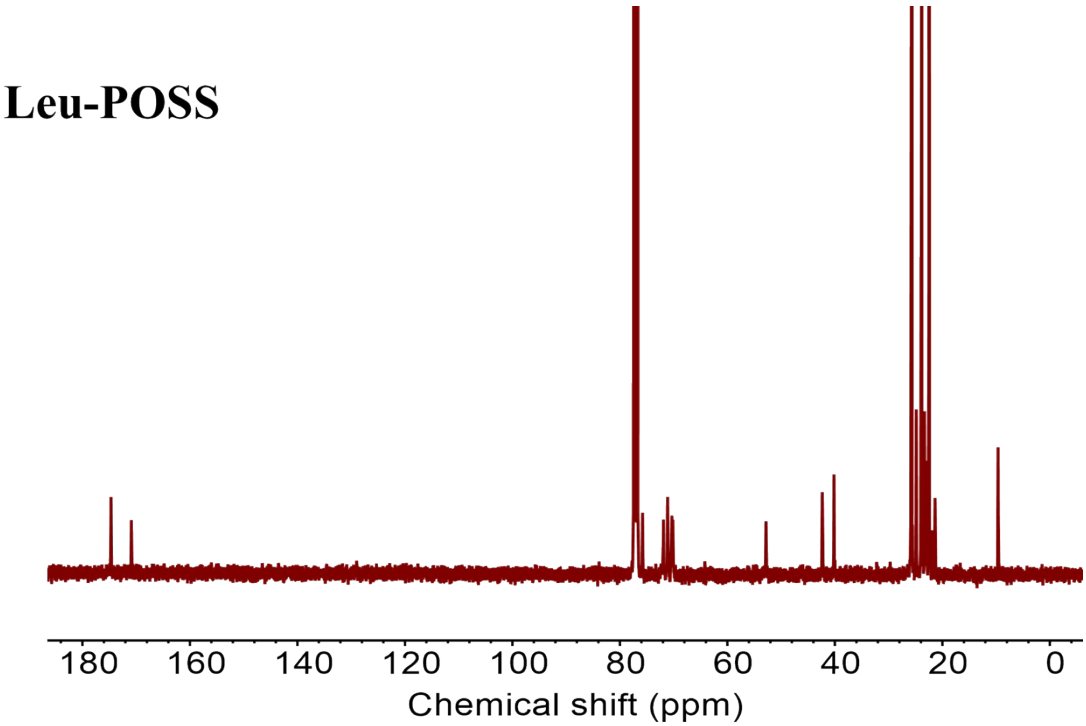

Figure S14. ^{13}C NMR spectrum of Leu-POSS.

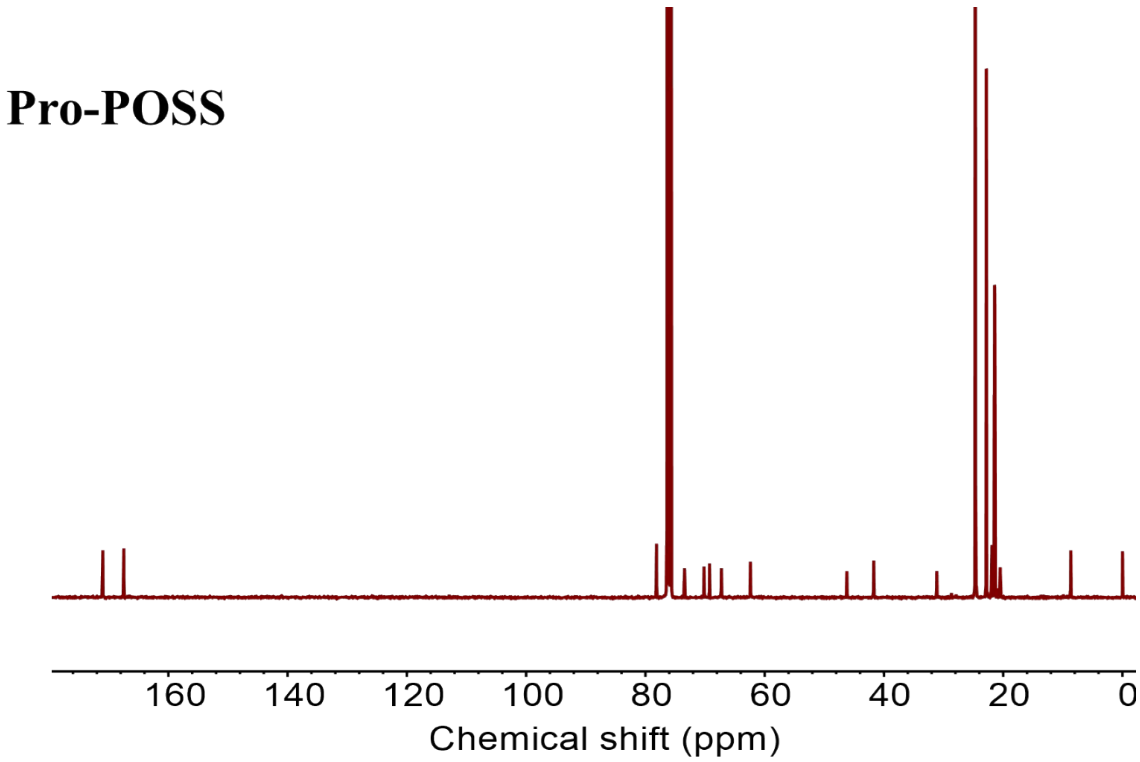

Figure S15. ^{13}C NMR spectrum of Pro-POSS.

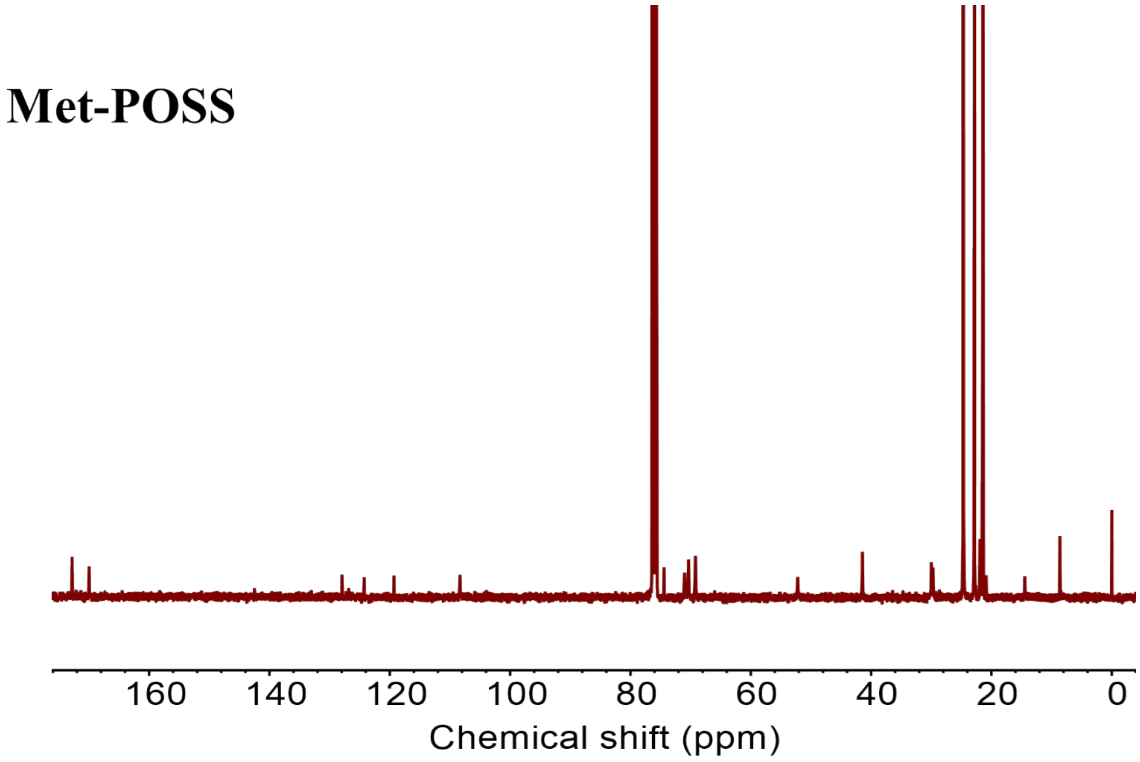

Figure S16. ^{13}C NMR spectrum of Met-POSS.

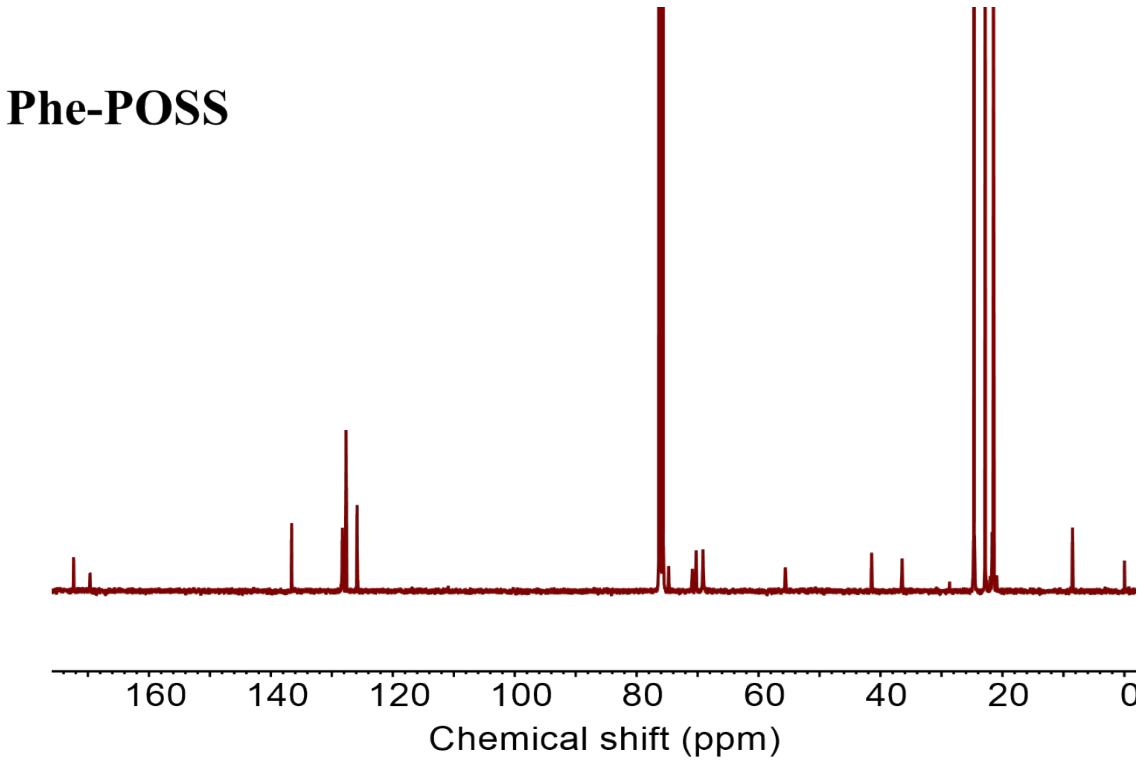

Figure S17. ^{13}C NMR spectrum of Phe-POSS.

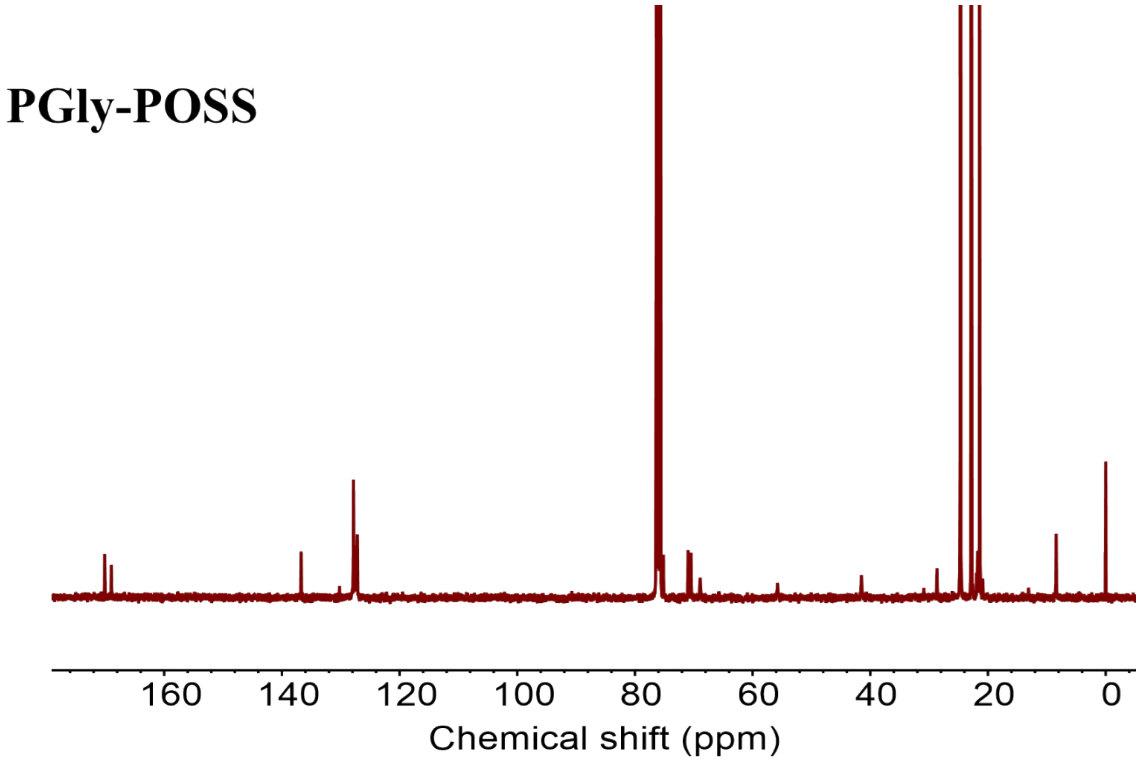

Figure S18. ^{13}C NMR spectrum of PGly-POSS.

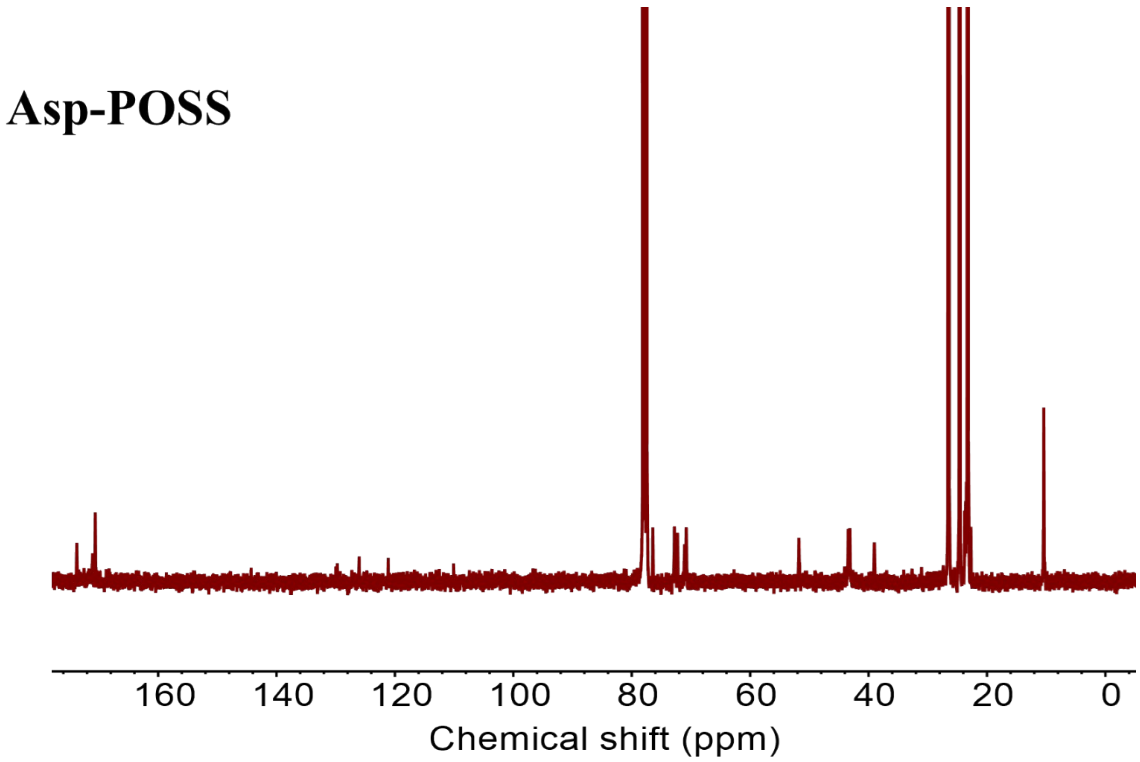

Figure S19. ^{13}C NMR spectrum of Asp-POSS.

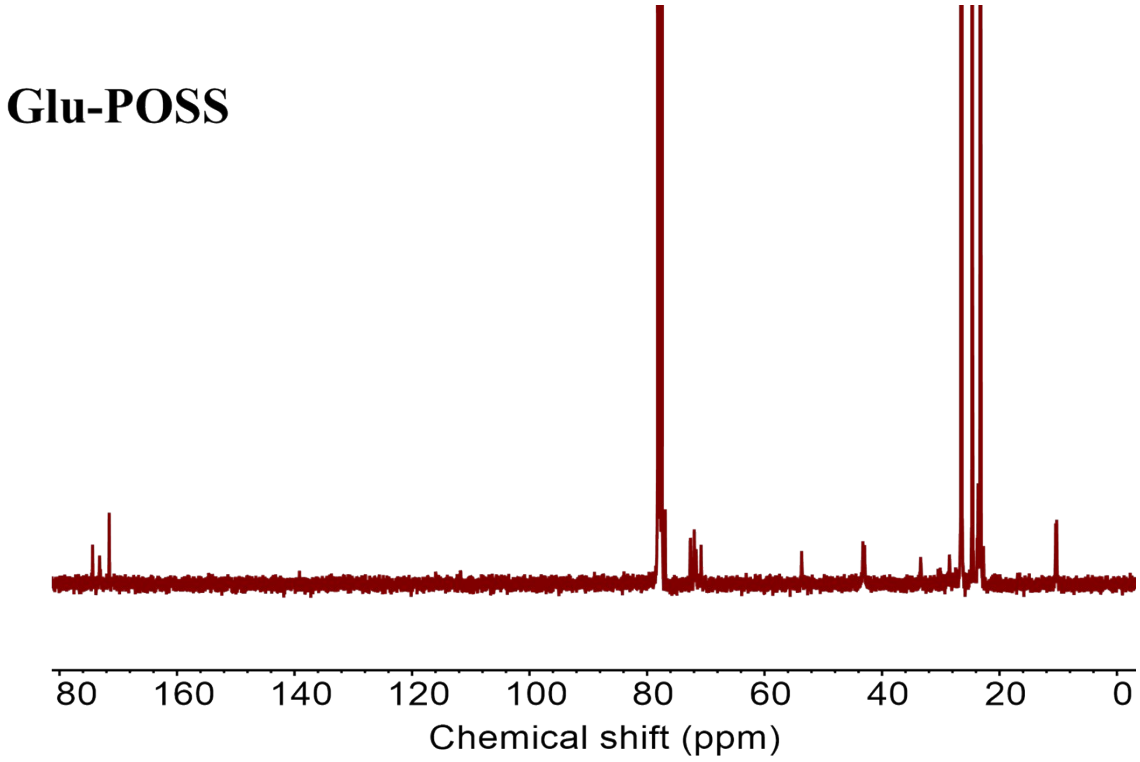

Figure S20. ^{13}C NMR spectrum of Glu-POSS.

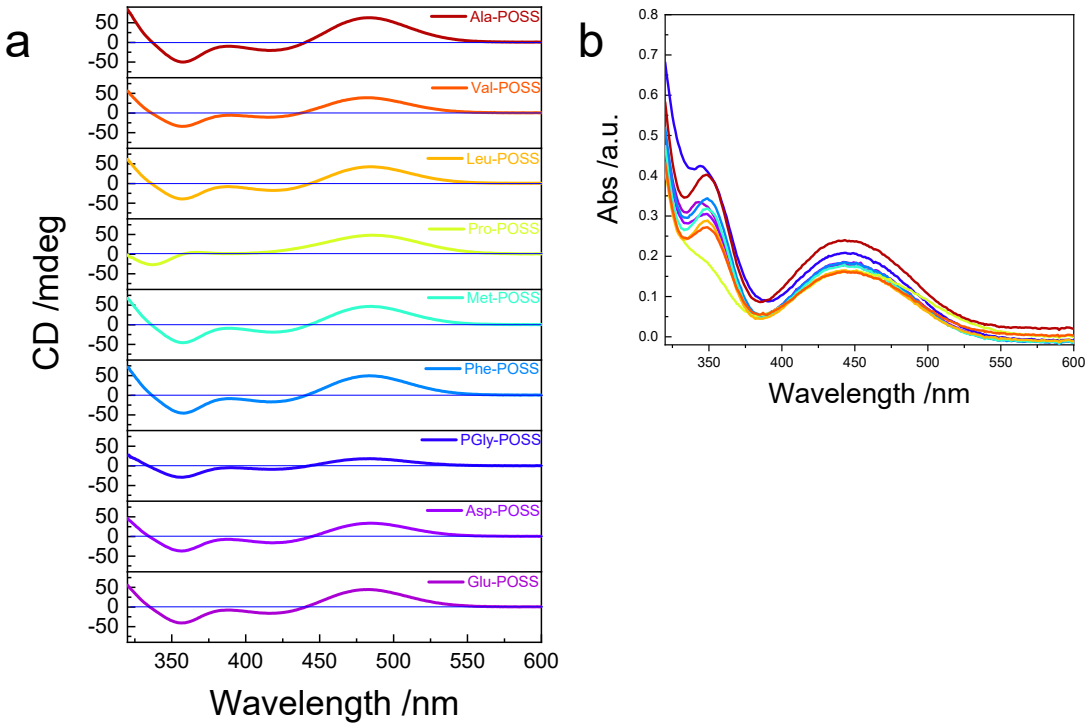

Figure S21. (a) CD spectra and (b) corresponding UV-vis spectra of POSS derivatives (1 mM, in $CHCl_3$)

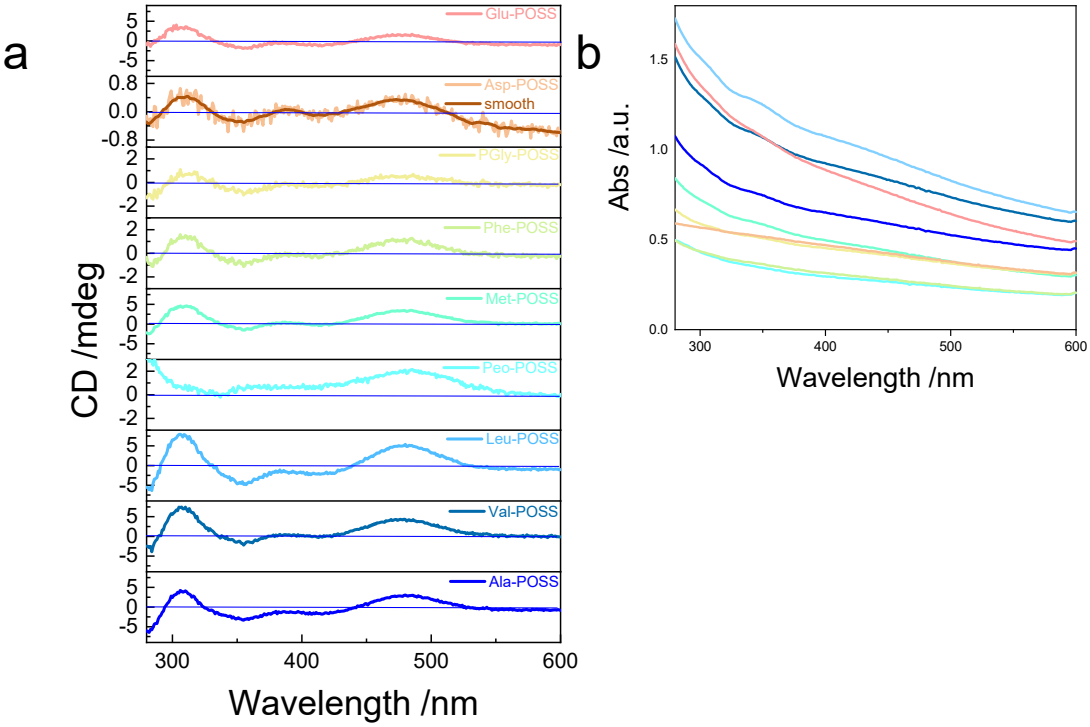

Figure S22. (a) Solid ECD spectra and (b) corresponding UV-vis spectra of POSS derivatives.

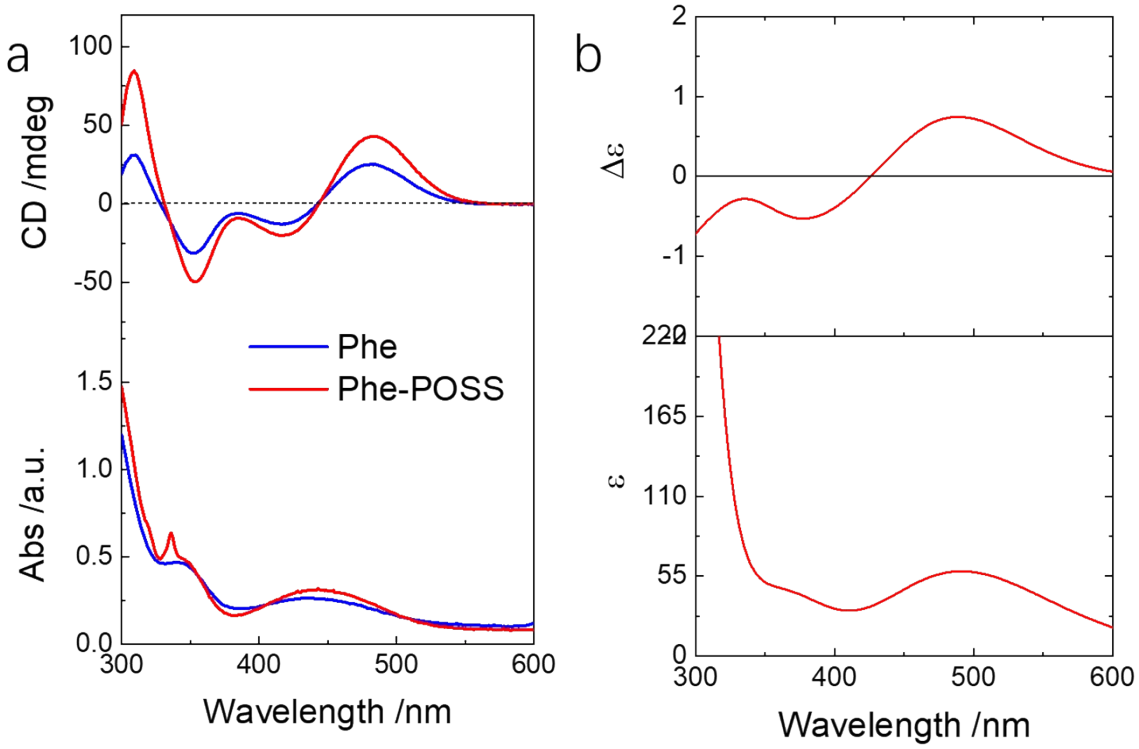

Figure S23. (a) Comparison of CD spectra between Phe (1,1'-ferrocenyl diphenylalanine) and Phe-POSS. (b) Calculated ECD spectra of Phe.

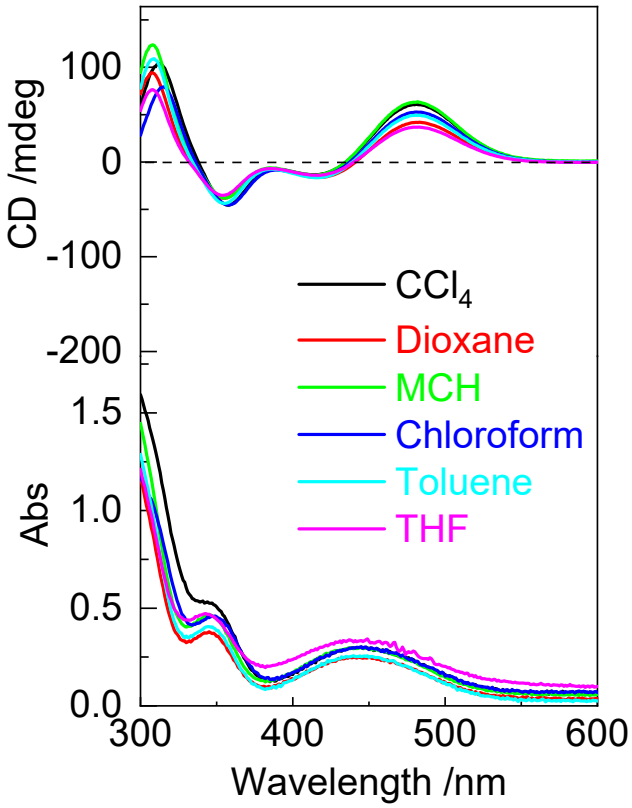

Figure S24. CD spectra of *L*-Val-POSS in different solvents (1 mM).

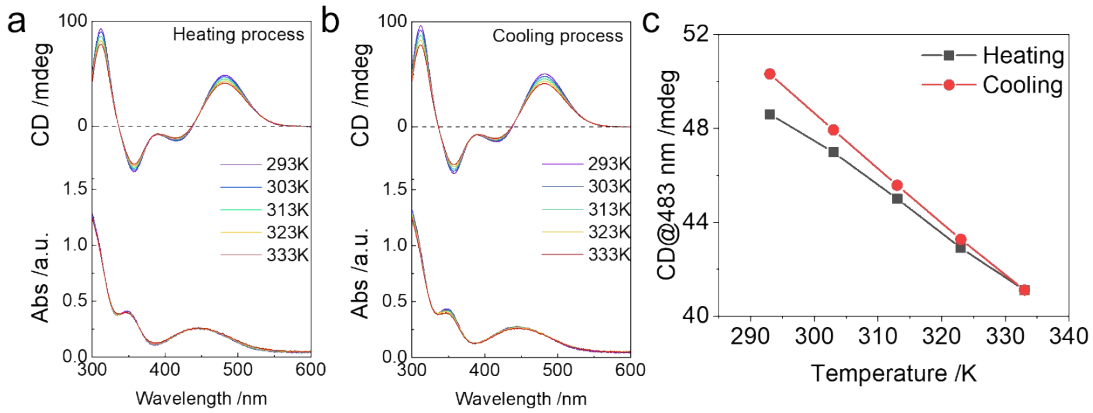

Figure S25. (a,b) Temperature-variable CD spectra of *L*-Val-POSS (1 mM) in the heating and cooling processes. (c) Corresponding CD intensity at 483 nm as a function of temperature.

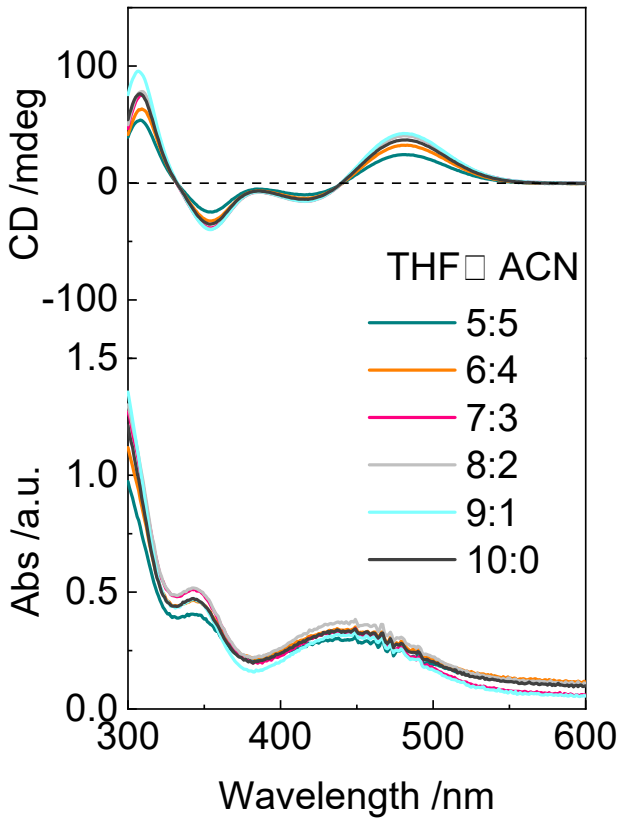

Figure S26. CD spectra of *L*-Val-POSS with different solvent ratios. When the fraction of ACN was higher than 50 vol%, precipitates shall be given. With increasing ACN fraction, no apparent correlation of CD signal and solvent fraction but irregularly changed Cotton effects were observed.

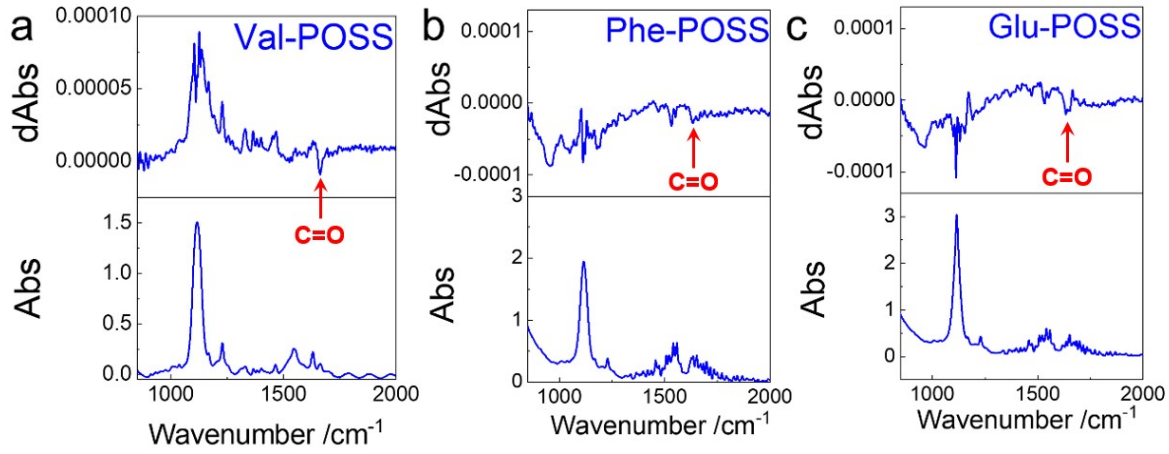

Figure S27. VCD spectra of (a) Val-POSS, (b) Phe-POSS, and (c) Glu-POSS (50 mg/mL in CCl_4).

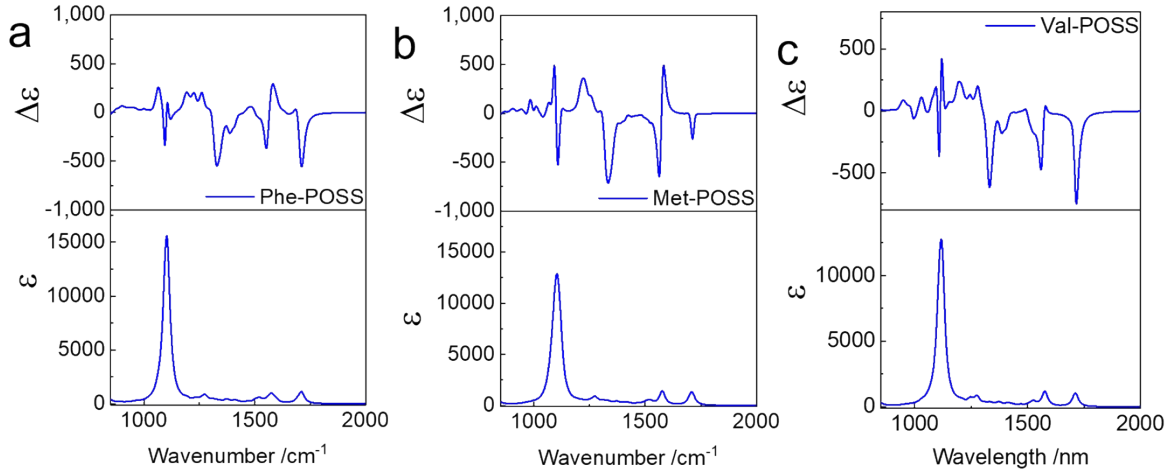

Figure S28. Simulated VCD spectra of (a) Phe-POSS, (b) Met-POSS and (c) Val-POSS (B3LYP/6-311g FWHM 15 cm^{-1}).

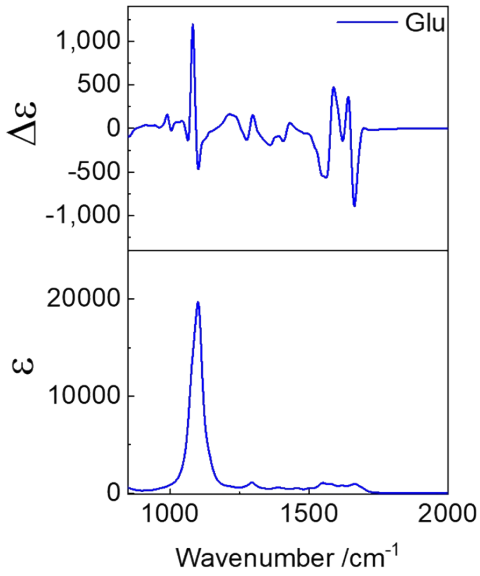

Figure S29. Simulated VCD spectra of Glu-POSS (B3LYP/6-31g FWHM 15 cm^{-1}).

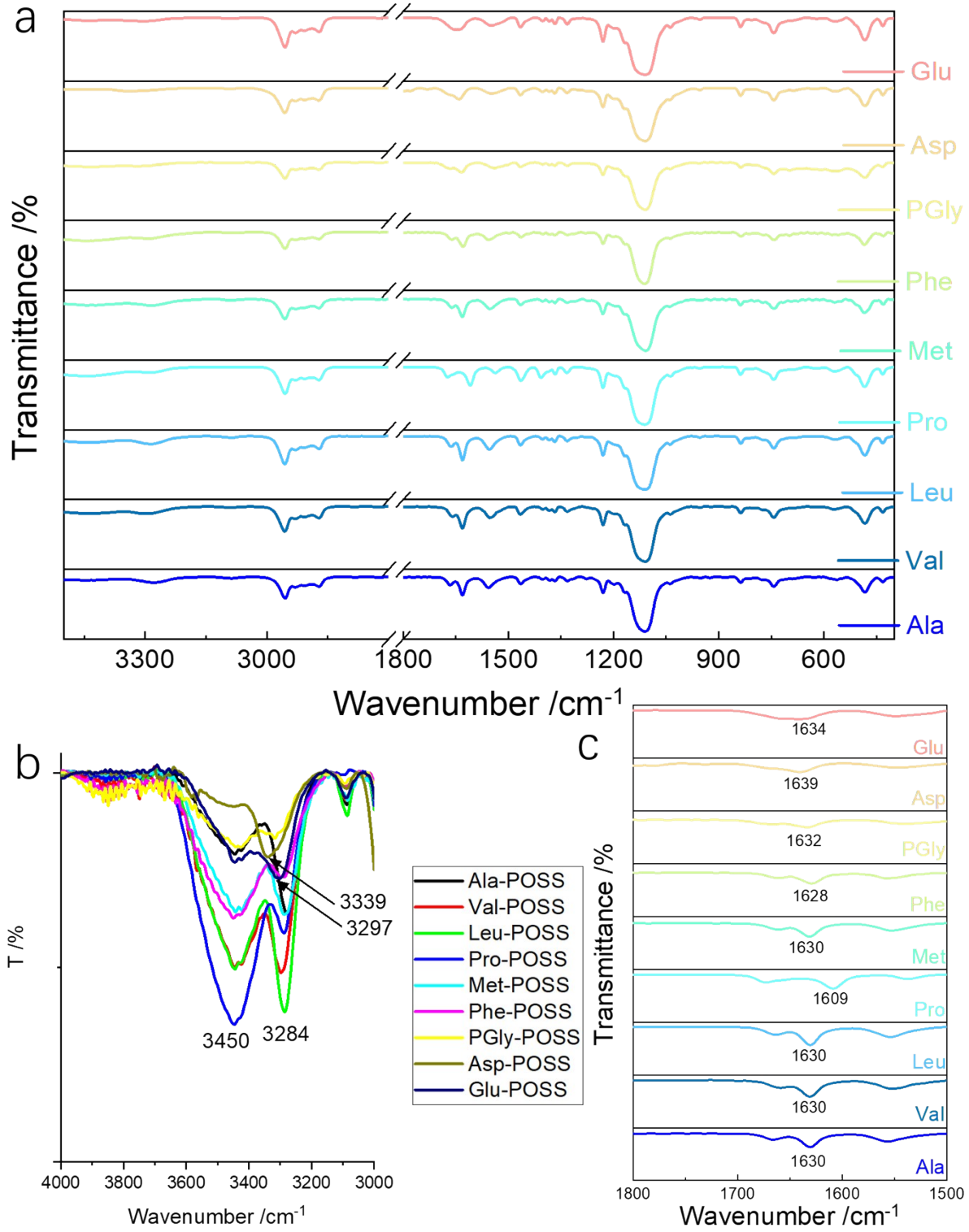

Figure S30. (a) FT-IR spectra of POSS derivatives. (b,c) Partial FT-IR spectra of each building units.

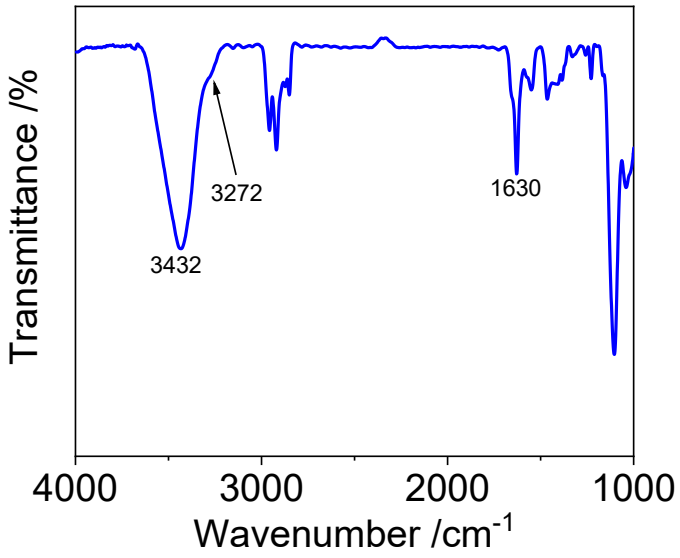

Figure S31. FT-IR spectrum of Val-POSS measured in liquid state (1 mM in CCl_4).

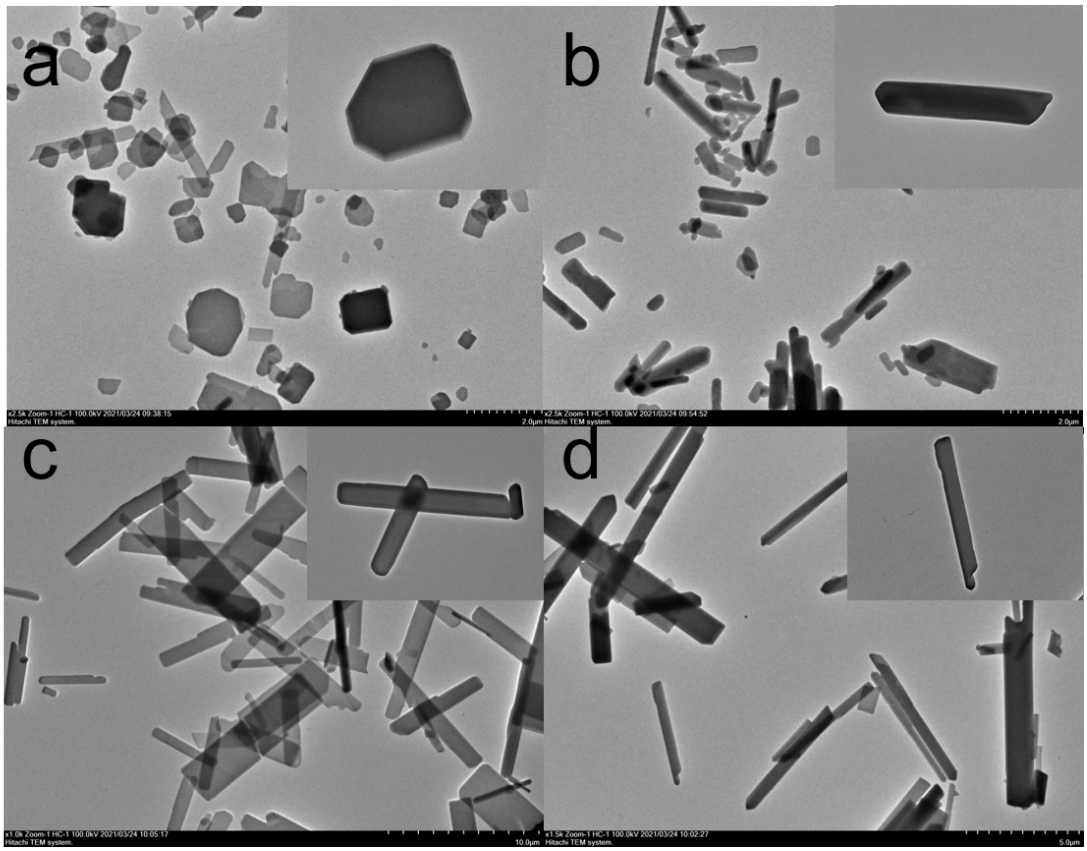

Figure S32. TEM image of (a) Ala-POSS, (b) Leu-POSS, (c) Phe-POSS, and (d) Met-POSS (1 mM, THF/MeCN 1/9).

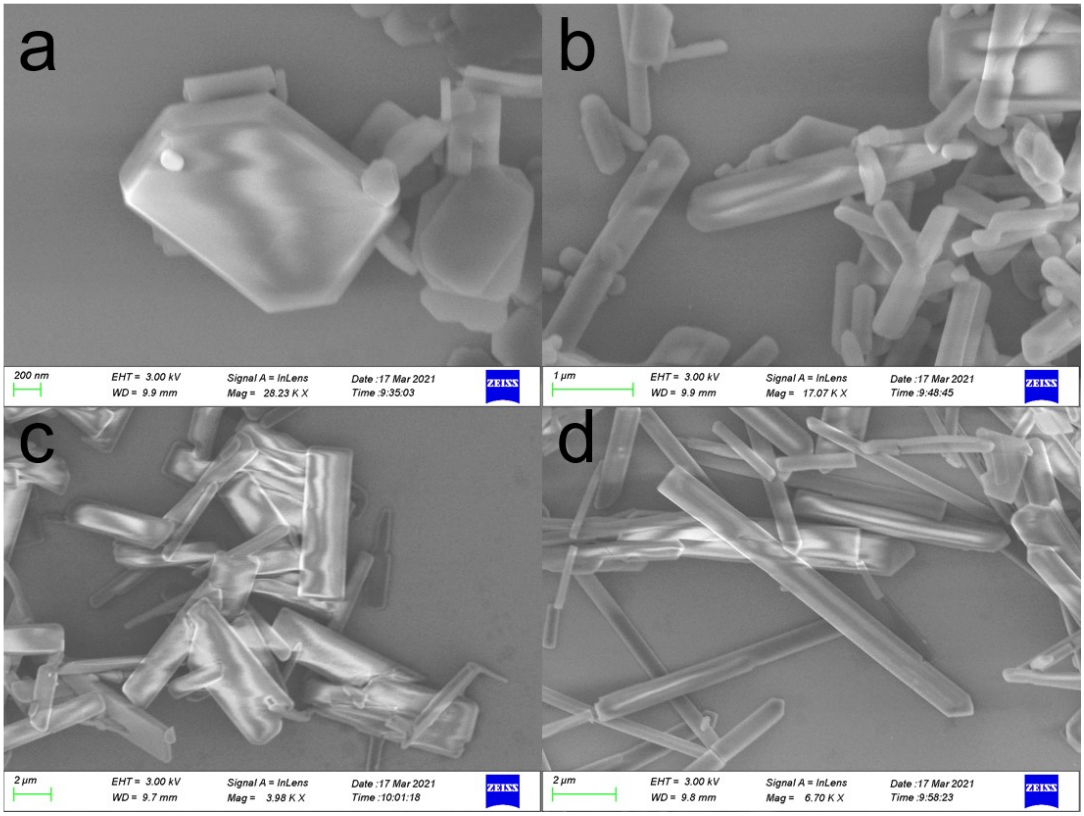

Figure S33. SEM image of (a) Ala-POSS, (b) Leu-POSS, (c) Phe-POSS, and (d) Met-POSS (1 mM, THF/MeCN 1/9).

Table S1. Crystal data of Phe-POSS.

Deposition Number	2096836
Formula	C_{92} H_{166} Fe N_4 O_{28} Si_{16}
Temperature(K)	293(2)
Wavelength	1.54184Å
Crystal system	orthorhombic
Space group	P 2_1 2_1 2_1
a,b,c/Å	**a** 16.2474(5) **b** 17.2899(8) **c** 46.6858(17)
V, Å3	13114.8
Cell angles	α 90 β 90 γ 90
Z, Z'	Z: 4 Z': 0
R-factor (%)	13.09

Table S2. Crystal data of Val-POSS.

Deposition Number	2096837
Formula	C_{84} H_{166} Fe N_4 O_{28} Si_{16},2(C_4 H_8 O_2)
Temperature(K)	173.00(10)
Wavelength	1.54184Å
Crystal system	monoclinic
Space group	P 2_1
a,b,c/Å	**a** 16.9205(5) **b** 17.5657(5) **c** 21.7093(5)
V, Å3	6451.5
Cell angles	α 90 β 90.980(2) γ 90
Z, Z'	Z: 2 Z': 0
R-factor (%)	10.84

Table S3. Crystal data of Met-POSS.

Deposition Number	2096838
Formula	C_{80} H_{156} Fe N_4 O_{27} S_2 Si_{16}, C_{71} H_{136} Fe N_4 O_{28} S Si_{16}, C_2 H_6 S
Temperature(K)	173.01(10)
Wavelength	1.54184Å
Crystal system	monoclinic
Space group	C2
a,b,c/Å	**a** 49.9932(14) **b** 17.2234(3) **c** 37.4731(9)
V, Å3	26797.5
Cell angles	α 90 β 123.849(3) γ 90
Z, Z'	Z: 8 Z': 0
R-factor (%)	13.41